TELEDETECCIÓN - Hacia un mejor entendimiento de la dinámica global y regional
Ed. Martin, 2007, ISBN: 978-987-543-126-3

Assessment of Terra-ASTER and Radarsat imagery for discrimination of dunes in the Valdes Peninsula: an object oriented approach

Blanco, Paula D.[1] [a]; Metternicht, Graciela I. [b]; del Valle, Héctor F.[a]; Sione, Walter[cd]

[(a)] Centro Nacional Patagónico-CONICET.
Boulevard Brown 2825, U9120ACF, Pto Madryn, Argentina
[(b)] School of Natural and Built Environments, University of South Australia,
5095, Mawson Lakes, SA
[(c)] CEREGeo-FCyT/UADER,
Ruta 11 Km 10, 3100, Oro Verde, Entre Ríos, Argentina
[(d)]PRODITEL-Universidad Nacional de Luján,
Cruce rutas ex. 5 y 7, 6700, Luján, Bs As, Argentina

RESUMEN

Areas como Península Valdés (SE Argentina), Patrimonio de la Humanidad desde 1999, están sujetas a degradación del suelo por acción eólica y sobrepastoreo. La cartografía de indicadores de degradación del paisaje, como dunas activas activas y estabilizadas, es crucial para mejorar la predicción, monitoreo y manejo de suelos afectados. Este trabajo compara clasificaciones basadas en el objeto y en el píxel para la discriminación de dunas activas y estabilizadas, y evalúa las diferencias en la fiabilidad de la clasificación al usar la sinergía de ASTER y Radarsat.

Palabras clave: Segmentación, Terra-ASTER, Radarsat-ASAR.

ABSTRACT

Areas like the Peninsula Valdes (SE Argentina), declared a World Heritage site in 1999, are subject soil degradation by wind and overgrazing. Mapping landscape degradation indicators such as stabilized and active dunes is critical to improve prediction, monitoring and planning of areas threatened by sand encroachment. To this end, this paper investigates the contribution of optical sensors like the Terra-ASTER and the microwave Radarsat ASAR to the discrimination of these land degradation features. Furthermore, two methods-per pixel and object-based classification-are explored and compared.

Keywords: Segmentation, Terra-ASTER, Radarsat-ASAR.

Introduction

Arid and semiarid drylands compose nearly a one-third of the land surface of the world (OIES, 1991). It is estimated that 50% to more than 70% of these areas are degraded as a result of overgrazing, aggravated by the characteristics of dryland climates (Warren & Agnew, 1988). Areas like Peninsula Valdes (southern Argentina), declared a UNESCO World Heritage site in 1999, are subject soil degradation by wind and overgrazing. Mapping and monitoring the presence of landscape degradation indicators such as stabilized and active dunes is crucial to improve prediction, and for monitoring and planning of areas threatened by sand encroachment. To this end, this research aims to: (1) map active and inactive dunes by using optical sensors like the Terra-ASTER; (2) assess accuracy improvements in the detection of dunes by incorporating microwave Radarsat SAR data; and (3) compare the results of a per pixel classification against an object-oriented approach for the of active and stabilized dunes.

[1] Contacto autor: Te: +54-2965- 451024/ Interno: 326 - Correo electrónico: blanco@cenpat.edu.ar

Satellite remote sensing is an effective tool for mapping landforms in a rapid and accurate manner. Visible-infrared (VIR) data can be used to discriminate active and stabilized dunes based on the distinctive reflectance values of light-colored sands (proper of active dune areas) and dark-colored vegetation, which produce significant tonal differences in the remote sensing imagery (e.g., Paisley et al., 1991). Synthetic Aperture Radar (SAR), in contrast to VIR, is an active form of remote sensing. Radar images have the potential to provide information on geometry of sand dunes and other aeolian features because the radar response to the structure of surficial features contrasts (Blumberg, 1998). Thus, by merging optical and radar, an additional portion of the spectrum is available which may improve classification.

Classification based on individual pixels is generally unsatisfactory for arid landforms, that often consist of highly variable mixtures of scattering objects and are largely distinguished by their spatial, besides their spectral, characteristics. Hence, much information is contained in the relationship between adjacent pixels, including shape, texture, relational and contextual information, which allows for identification of individual objects as opposed to single pixels (Thomas et al., 2003). Pixels are aggregated into image objects by segmentation, which is defined as the division of remotely sensed images into discrete regions or objects that are homogenous with regard to spatial or spectral characteristics (Ryherd & Woodcock, 1996). Object-based segmentation and image classification techniques are receiving increasing attention for widespread application to classification of spectral and SAR data (e.g., Laliberte et al., 2007).

Methodology

Study area

Our study was conducted in Península Valdés (lat 42º32'S, 63º54'W), Patagonia argentina (Fig. 1). Climate is semiarid, with an annual mean temperature of 13ºC and average annual rainfall of 231 m). Mean annual wind speed is 25 $km \cdot h^{-1}$,the prevailing winds are from the west and north-west.

Two dunefields are distinguishable in Península Valdés: the largest one is in the central area forming a belt that stretches from the west to the east coast, and the smaller one is a fringe-like dunefield in the southwest corner of the peninsula. General features in the topography of the dunefield are relic aeolian landforms, megapatches of active sand dunes and erosional

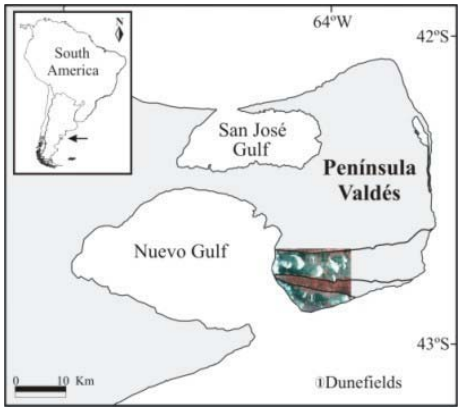

Fig. 1. Study area location. ASTER composite, bands 3, 2, 1

features like regs and blowouts. Megapatches of active sand dunes include barchan, dome and transverse dunes. Relict aeolian landforms include sand sheets and lineal dunes stabilized by psammophile species.

The vegetation is transitional between Monte and Patagonian Phytogeographic Provinces (León et al., 1998). The vegetation cover is 50-80% on the dunefields, the most widespread communities are grasslands of *Sporobolus rigens, Panicum urvilleanum* and *Stipa tenuis;* and scrublands dominated by *Hyalis argentea*. A shrub steppe of *Chuquiraga avellanedae* extends between both dunefields, but this area were not including in this study.

Using pre-existing physiographic and vegetation maps, and information on current field situation, six dominant vegetation-landforms patterns were identified in the study area. These are: Active dune, Reg, Grassland, Grass Stabilized Lineal Dune, Scrubland, and Scrub Stabilized Lineal Dune.

Research approach

The research approach encompasses:

1) Identification of landscape features related to the presence of active and stabilized dunes. Two vegetation types are considered as dune stabilizers: scrub and grass;
2) Calibration and georeferencing of the Terra ASTER imagery, including the computation of spectral indices and principal component analysis for the removal of redundant spectral information;
3) Despeckle and georeferencing of a precision mode Radarsat imagery;

4) Creation of a geo-spatial soil database to store field observations and spectral characteristics of wind-erosion related features in the optical and microwave regions of the spectrum;
5) Extraction of Radarsat derived textural measures;
6) Classification of the selected imagery using a per-pixel maximum likelihood algorithm in ERDAS Imagine software.
7) Segmentation and object-oriented classification using eCognition software.
8) Accuracy evaluation of the resulting classifications using error matrices and Kappa statistics.

Image preprocessing

ASTER level 1B scene was acquired on 27th November 2004, georeferenced in the UTM projection, WGS-84 ellipsoid, and converted to radiance values. ASTER acquires data in 3 separate subsystems: VNIR (bands 1, 2, 3, SR=15 m), SWIR (bands 4-10, SR=30 m), and TIR (bands 11-14, SR=90 m). Given the high correlation between bands (above 0.9) a PCA was applied to remove redundant information. The first two components explained 98% of the image variability, and thus they were selected for further analysis. The ASTER VNIR and band 4 showed the highest contribution to these first two components, and thus were selected as the raw bands to be included in the classification process. The Soil Adjusted Vegetation Index (SAVI) was computed as a means to gather information on vegetation cover. SAVI (similar to NDVI with an L factor to compensate for vegetation density) is recommended for sparsely vegetated areas (Huete, 1998).

Radarsat-1 ASAR image, C-band, HH polarization was acquired on the 1st January 2005, in fine mode 4 with a spatial resolution of 8 m (Fig. 2). The raw data was converted to magnitud image products, filtered to decrease speckle contribution (Frost filter) and georeferenced. Textural measures derived from the Grey Level Co-occurrence Matrix (GLCM) were used ascertain their value for mapping active and stabilized dunes (Haralick, 1973). Measures of mean, variance, contrast, and dissimilarity were implemented in the Radarsat imagery

Subsequently, image to image registration was conducted between the ASTER and Radarsat images in order to keep registration errors to less than half a pixel. To this end, a nearest neighbour resampling algorithm and output pixel size of 8 m were used. Bands 1-4 from ASTER and the selected Radarsat-derived texture measures were stacked into one single image for the multisensor analysis (ERDAS, 2003).

Fig. 2. Radarsat-1 SAR image showing part of the study area. The brightness tones represent backscatter magnitud values

Pixel based classification

For the pixel based classification standard maximum likelihood classificator as featured by the software Erdas Imagine was used. The functionality of the pixel-based classification is not explained here in detail and can be found in all standard literature (Chuvieco, 2002).

Object-oriented approach

The procedure as outlined in Figure 3 can be divided into two major parts. First, the multi-segmentation of the input data is performed. This procedure produces highly homogeneous segments in a selectable resolution and of a comparable size. Classification is then performed using those objects rather than single pixels. The classification of the image objects can be performed by using nearest neighbour classifiers based on user selected samples or by using fuzzy membership functions (Zadeh, 1965), with user-defined rules. A fuzzy membership ranges from 0 to 1 for each object's feature values with regard to the object's assigned class. Spectral, shape, and statistical characteristics as well as relationships between linked levels of the image objects can be used in the rule base to combine objects into meaningful classes (Benz et al. 2004).

Two image segmentation trials were implemented using different input data sets (Table 1).The first trial used the four raw ASTER bands (1 to 4); whereas the second integrated spectral and texture information (i.e. mean, variance, contrast and dissimilarity co-ocurrence texture

images) derived from Radarsat data. The object oriented approach considers three parameters for image segmentation scale, colour/shape ratio, and smoothness/compactness ratio. The weights for color and shape was established after several iterations to a ratio of 0.8:0.2 for the relative importance of color versus shape and 0.1:0.9 for compactness versus smoothness.

Table 1. Input datasets used in the trials

Inputs	Scale		
	Level 1	Level 2	Level 3
B1-4 ASTER	3	7	9
ASTER & Textural Data	8	15	25

The image classification followed a three-levels approach (Figure 4), whereby the third level, segmented on the coarse scale, used a SAVI threshold for separation of broader land covers (e.g. objects with a SAVI less than 0.74 were considered to be dune fields; above 0.74 were classed as *Shrub Steppe*). A separation between *Grassland*, *Scrubland* and *Areas Not-Vegetated* classes was achieved by a nearest neighbour classification, based on the training chosen in the SAVI feature space.The second level aimed at identifying active dunes by defining fuzzy membership functions for mean brightness values, related to the input data of each trial (Table 1). Two subclasses of the *Active Dune*, namely *AD-1* and *AD-border*, were defined. Then, an object fusion was applied to group the objects of these classes under the general class, active dunes. The *Reg* class was considered complementary to actives dunes.

Lastly, the first level was designed to extract areas of stabilized dunes. To this end, we discriminated between dunes stabilized by grass and dunes fixed by scrub, defining the classes *GSD*-1 and *SSD*-1 based on membership functions for mean brightness values. Because these classes had similar brightness values and could be confused with other classes, we established a restriction on the shape of the segments: the length/width ratio should be bigger than 4. In order to integrate wrongly excluded objects two new subclasses were defined, *GSD-border* and *SSD-border*, which had the brightness feature space broader but with the constraint that the relative border length to *GSD-1* and *SSD-1*, respectivaly, was greater than 1. The *Grassland* and *Scrubland* classes were defined as complementary of those classes, respectively.

Accuracy assessment

The accuracy assessment was done by means of an error matrix based on stratified and randomly selected sites across the study area. The ground truthing was carried out by field survey in the summer of 2005 visiting as many sites as possible, and confirming the vegetation-landform type in situ with a Global Positioning System (GPS) unit. At each validation site, an area at 45 by 45 m was examined, to account for location errors caused by positional inaccuracies of the GPS and/or the geometric correction of the satellite imagery. The number of validation pixels was 729 for *Active Dune,* 414 for *Reg*, 369 for *Grassland*, 360 for *Scrubland*, and 837 and 792 for *Lineal Dunes Stabilized* by *Grass* and *Scrub*, respectively.

The error matrix was used as the basis for calculating the overall accuracy, individual class user´s and producer´s accuracy, KHAT statistic and its variance (an estimate of the kappa coefficient) (Congalton, 1991). The efficiency of the synergistic approach was evaluated with a kappa analysis. KHAT statistic and its variance were used to construct a hypothesis test for statistically significant difference between error matrices (Cohen, 1960), being the null hypothesis that there is no disagreement between the KHAT values.

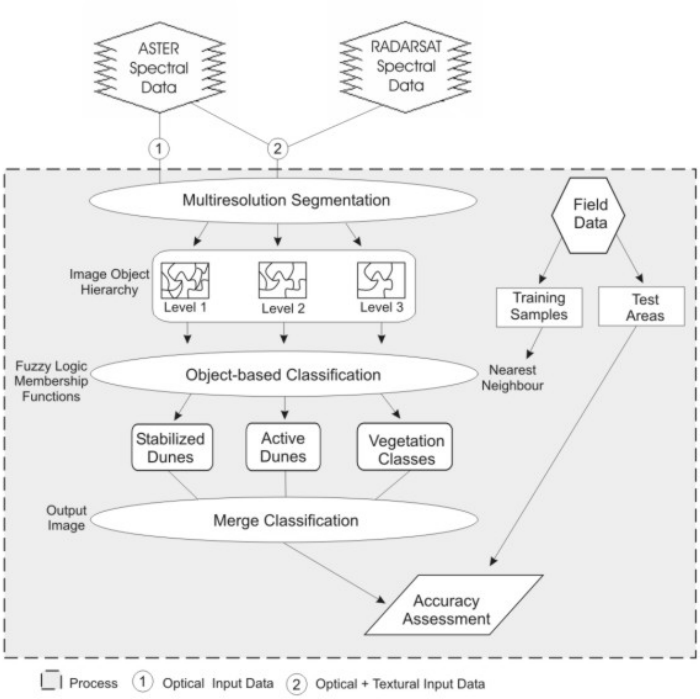

Fig. 3. Conceptual model of the object oriented approach adopted in this study.

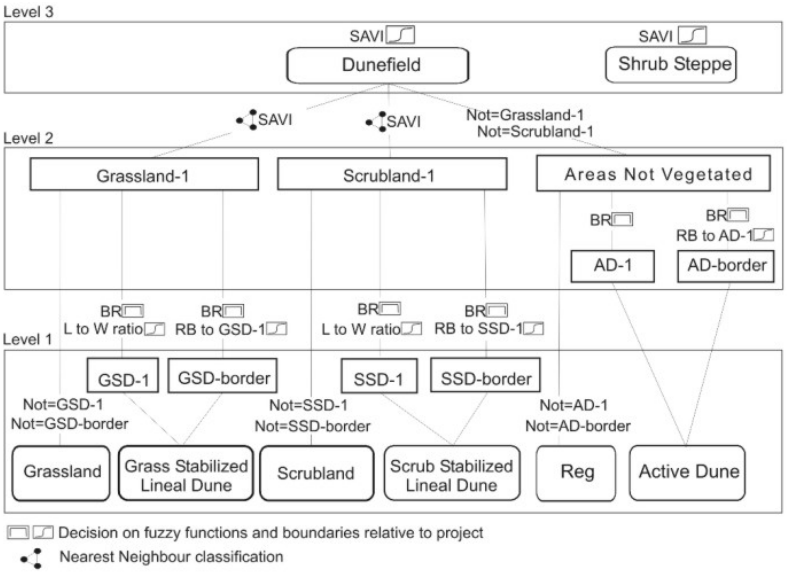

Fig. 4. Fuzzy membership functions for all the classes. BR denotes brightness, L to W means the ratio Length/Width and RB is the relation of border to a certain class.

Initial results

Per pixel classification of the ASTER data

The first step was to analyze the separability of the classes of interest using a maximum likelihood classifier as featured in the *ERDAS Imagine* software. The scatter plot (Fig. 5) shows significant overlaps between the classes *Active Dune* and *Reg*, as well as *Grassland* and *GSD*, and between *Scrubland* and *GSD* .

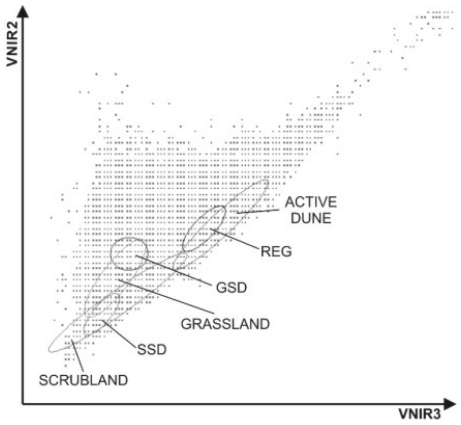

Fig. 5 Scatter plot of the maximum likelihood classification.

These results are consistent with the classification outputs shown in Fig. 6. The ASTER spectral signatures for the lineal dunes and the vegetation types do not differ greatly, returning visually and spectrally similar responses. They have similar average DNs and all possess high standard deviations. This creates areas of overlap in their spectral signatures, which creates confusion, and limits their spectral separability. The class *Active Dune* shows a higher average DN, which improves its spectral discrimination from the inactive dunes, though exhibiting a high standard deviation with areas of overlap with *Reg* class.

The final classification result has an overall accuracy of 52.7%, and a KHAT equal to 43.4%. According to Congalton (1991) kappa values can be subdivided into 3 groups, where a value greater than 0.80 (80%) represents strong agreement, a value between 0.40 and 0.80 (40 to 80%) represents moderate agreement, and a value below 0.40 (40%) represents poor agreement. Adopting this standard, the accuracy achieved by the per pixel classification represents a moderate agreement. Both the user's and producer's accuracies for the classes were low too (results are not shown), as they had nearly the same number of pixels confused with the other classes as they have correctly classified.

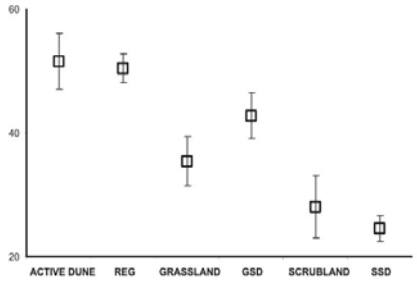

Fig. 6 Spectral signatures of the different classes for VNIR1-band, ASTER scene.

Object-oriented classifications

The high standard deviation associated with the ASTER classes suggests that measures of image texture may increase the discriminatory ability of the optical sensor. Figures 7 and 8 show the results of using object-oriented classifications based in optical data from ASTER, and spectral plus textural image information, respectively.

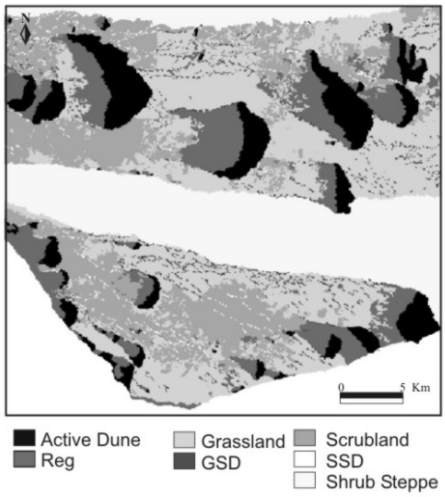

Fig. 7. Cartography object-oriented of soil degradation indicators using ASTER data.

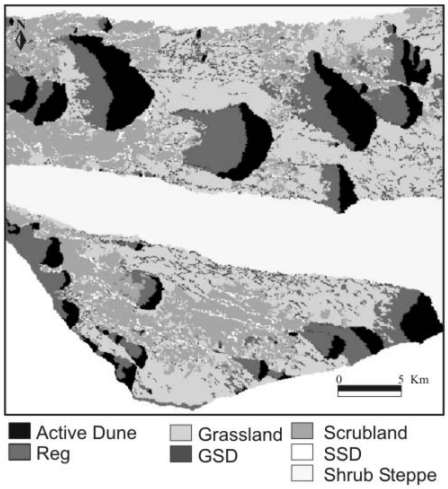

Fig. 8. Object-oriented cartography of soil degradation indicators using the fusion of ASTER and Radarsat-derived textural data.

Accuracy assessments for ASTER alone and ASTER combined texture maps are presented in table 2 and 3, respectively. The KAPPA analysis result for the pairwise comparison between the ASTER and ASTER combined texture maps shows a result of 5.96, which is superior than 1.96 (the critical value at the 95% confidence level) revealing that the two error matrices are significantly different.

Kappa statistics above 80%, with 3 classes showing above 90% accuracy of discrimination, are achieved when mapping the six classes of interest using the synergy of spectral and textural data derived from ASTER and Radarsat imagery (Table 3). A comparison of the classification accuracies obtained with the different layer combinations revealed that the ASTER combined texture had better overall accuracy and a higher KHAT statistic value than the classifications resulting of ASTER layer inputs, implying that the synergistic approach enabled better discrimination of the land degradation features in the study area.

These initial results suggest an improvement in the classification of active dunes and stabilized dunes (vegetated by either scrub or grass) is achieved by using an object-oriented classification that integrates textural information derived from microwave imagery and optical/IR data from Terra-ASTER. It appears that changes in surface roughness caused by different vegetation types stabilizing the dunes is a major influence in radar backscattering. For instance, Radarsat imagery enables a clear separation of long and narrow dunes stabilized by scrub against those stabilized by grass, the former showing a higher classification accuracy. On the other hand, ASTER optical and infrared wavebands show superior performance in the cartography of grass-stabilized dunes. It also appears that the synergistic use of microwave, optical and infrared data increases substantially the accuracy in the discrimination and mapping of soil degradation features related to wind erosion.

Table 2. Accuracy assessment of the ASTER object-oriented classification.

Classes	ASTER data input		
	PA (%)	UA (%)	KHAT
Active Dune	91	95	89
Reg	87	77	85
Grassland	88	68	86
GSD	79	94	73
Scrubland	92	59	91
SSD	70	95	64
Overall	OA 82.8%		KHAT 79.1%

Table 3. Accuracy assessment of the combined ASTER-Radarsat derived textural data classified using an object-oriented approach.

Classes	ASTER & textural data input		
	PA (%)	UA (%)	KHAT
Active Dune	94	95	92
Reg	91	82	90
Grassland	83	77	81
GSD	87	92	83
Scrubland	95	83	94
SSD	87	98	86
Overall	OA 89.7%		KHAT 87.4%

Acknowledgments

This study was funded by CONICET (PIP-2004, N° 6413) and FONCyT (BID 1728/OC-AR PICTR/03 Nº 439). Comisión Nacional de Actividades Espaciales (CONAE) supplied the Terra-ASTER and Radarsat-1 ASAR images, within the framework of the project to promote monitoring of World Heritage sites (UNESCO). We thanks to PRODITEL-Universidad Nacional

de Lujan for facilitating the eCognition software, and the Department of Spatial Sciences, Curtin University of Technology, where the leading author spent three months in research.

References

Benz, U.C., Hoffmann, P., Willhauck, G., Lingenfelder, I., Heynen, M. 2004. Multi-resolution, object-oriented fuzzy analysis of remote sensing data for GIS-ready information, ISPRS Journal of Photogrammetry and Remote Sensing, 58:239–258.

Blumberg, D.G., 1998. Remote sensing of desert dune forms by polarimetric synthetic aperture radar (SAR). Remote Sensing of Environment, 65:204– 216.

Chuvieco, E., 2002. Teledetección Ambiental: La observación de la Tierra desde el Espacio. Barcelona:Ariel Ciencia.

Cohen, J. 1960. A coeficient of agreement for nominal scales. Educational and Psychological Measurement, 1:37-40.

Congalton, R. 1991. A Review of Assessing the Accuracy of Classifications of Remotely Sensed Data. Remote Sensing of Environment 37:35-46.

ERDAS INC. 2003. ERDAS, Version 8.7. Available at: http://www.erdas.com/.

Haralick, R. M., Shanmugam, K., Dinstein, I., 1973. Texture feature for image classification. IEEE Transactions on Systems, Man, and Cybernetics, 3:610- 621.

Huete, A.R., 1988. A soil-adjusted vegetation index (SAVI), Remote Sensing of Environment, 25:295-309.

Laliberte A. S., Fredrickson, E. L., Rango, A., 2007. Combining decision trees with hierarchical object-oriented image analysis for mapping arid rangelands. Photogrammetric engineering & Remote sensing. 2:197-207.

Leon, R.J.C., Bran, D., Collantes, M., Paruelo, J.M., Soriano, A., 1998. Grandes unidades de vegetación de Patagonia extra andina. Ecología Austral. 8:75-308.

OIES, 1991. Arid ecosystem interactions. Boulder, CO: Office of Interdisciplinary Earth Studios.

Paisley, E.C.I., Lancaster, N., Gaddis, L.R., Greelye, R., 1991. Discrimination of active and inactive sand from remote sensing: Kelso Dunes, Mojave Desert, California. Remote Sensing of Environment, 37:153–166.

Ryherd, S., Woodcock, C. E., 1996. Combining spectral and texture data in the segmentation of remotely sensed images. Photogrammetric Engineering and Remote Sensing, 62:181–194.

Thomas, N., Hendrix, C., Congalton, R. G., 2003. A comparison of urban mapping methods using high-resolution digital imagery. Photogrammetric Engineering and Remote Sensing, 69: 963– 972.

Warren, A., Agnew, C., 1988. An assessment of desertification and land degradation in arid and semi-arid areas. Drylands Programme Research. Paper No.2. London: IIED.

Zadeh, L.,1965. Fuzzy sets. Information Control, 8:338–353.